Discontinuous Euler instability in nanoelectromechanical systems

Guillaume Weick,[1,2] Fabio Pistolesi,[3,4] Eros Mariani,[1,5] and Felix von Oppen[1]

[1]*Dahlem Center for Complex Quantum Systems and Fachbereich Physik, Freie Universität Berlin, D-14195 Berlin, Germany*
[2]*IPCMS (UMR 7504), CNRS and Université de Strasbourg, F-67034 Strasbourg, France*
[3]*CPMOH (UMR 5798), CNRS and Université de Bordeaux I, F-33405 Talence, France*
[4]*LPMMC (UMR 5493), CNRS and Université Joseph Fourier, F-38042 Grenoble, France*
[5]*School of Physics, University of Exeter, Stocker Road, Exeter, EX4 4QL, UK*

We investigate nanoelectromechanical systems near mechanical instabilities. We show that, quite generally, the interaction between the electronic and the vibronic degrees of freedom can be accounted for essentially exactly when the instability is continuous. We apply our general framework to the Euler buckling instability and find that the interaction between electronic and vibronic degrees of freedom qualitatively affects the mechanical instability, turning it into a discontinuous one in close analogy with tricritical points in the Landau theory of phase transitions.

I. INTRODUCTION

The buckling of an elastic rod by a longitudinal compression force F applied to its two ends constitutes the paradigm of a mechanical instability, called buckling instability.[1] It was first studied by Euler in 1744 while investigating the maximal load that a column can sustain.[2] As long as F stays below a critical force F_c, the rod remains straight while for $F > F_c$ it buckles, as sketched in Figs. 1(a) and 1(b). The transition between the two states is continuous and the frequency of the fundamental bending mode vanishes at the instability.

There has been much recent interest in exploring buckling instabilities in nanomechanical systems. In the quest to understand the remarkable mechanical properties of nanotubes,[3–5] there have been observations of compressive buckling instabilities in this system.[6] The Euler buckling instability has been observed in SiO_2 nanobeams and shown to obey continuum elasticity theory.[7] There are also close relations with the recently observed wrinkling[8] and possibly with the rippling[9] of suspended graphene samples. Theoretical works have studied the quantum properties of nanobeams near the Euler instability,[10–13] proposing this system to explore zero-point fluctuations of a mechanical mode[11] or to serve as a mechanical qubit.[13]

In this work, we study the interaction of current flow with the vibrational motion near such continuous mechanical instabilities which constitutes a fundamental issue of nanoelectromechanics.[14] Remarkably, we find that under quite general conditions, this problem admits an essentially exact solution due to the continuity of the instability and the consequent vanishing of the vibronic frequency at the transition ("critical slowing down"). In fact, the vanishing of the frequency implies that the mechanical motion becomes slow compared to the electronic dynamics and an appropriate non-equilibrium Born-Oppenheimer (NEBO) approximation becomes asymptotically exact near the transition. Here, we illustrate our general framework by applying it to the nanoelectromechanics of the Euler instability.

We find that the interplay of electronic transport and the mechanical instability causes significant qualitative changes both in the nature of the buckling and in the transport properties. In leading order, the NEBO approximation yields a current-induced conservative force acting on the vibronic mode. At this order, our principal conclusion is that the coupling to the electronic dynamics can change the nature of the buckling instability from a continuous to a discontinuous transition which is closely analogous to tricritical behavior in the Landau theory of phase transitions. Including, in addition, the fluctuations of the current-induced force as well as the corresponding dissipation leads to Langevin dynamics of the vibrational mode which becomes important in the vicinity of the discontinuous transition. Employing the same NEBO limit to deduce the electronic current, we find that the buckling instability induces a current blockade over a wide range of parameters. This is a manifestation of the Franck-Condon blockade[15–17] whenever the buckling instability remains continuous but is caused by a novel tricritical blockade when the instability is discontinuous. The emergence of a current blockade in the buckled state suggests that our setup could, in principle, serve as a mechanically controlled switching device.

II. MODEL

Close to the Euler instability, the frequency of the fundamental bending mode of the beam approaches zero while all higher modes have a finite frequency.[1] This allows us to retain only the fundamental mode of amplitude X [see Figs.
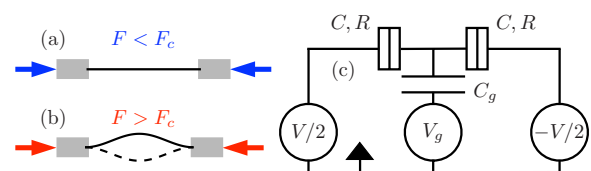

FIG. 1. (Color online) Sketch of a nanobeam (a) in the flat state and (b) the buckled state with two equivalent metastable positions of the rod (solid and dashed lines). An equivalent circuit of the embedded SET is shown in (c).

1(a) and 1(b)], and following previous studies[10–12] we reduce the vibrational Hamiltonian to[18]

$$H_{\text{vib}} = \frac{P^2}{2m} + \frac{m\omega^2}{2}X^2 + \frac{\alpha}{4}X^4, \qquad (1)$$

which is closely analogous to the Landau theory of continuous phase transitions. In Eq. (1), P is the momentum conjugate to X and m denotes an effective mass. The mode frequency $\omega^2 \sim 1 - F/F_c$ changes sign when F reaches a critical force F_c. Global stability then requires a quartic term with $\alpha > 0$. Thus, for $F < F_c$ ($\omega^2 > 0$), $X=0$ is the only stable minimum and the beam remains straight. For $F > F_c$ ($\omega^2 < 0$), the beam buckles into one of the two minima at $\pm X_+ = \pm\sqrt{-m\omega^2/\alpha}$.

The vibronic mode of the nanobeam interacts with an embedded metallic single-electron transistor (SET), consisting of a small metallic island coupled to source, drain, and gate electrode [Fig. 1(c)]. We assume that the SET operates in the Coulomb-blockade regime[19] and that bias and gate voltages are tuned to the vicinity of the conducting region between SET states with, say, zero and one excess electron. The electronic degrees of freedom couple to the vibronic motion through the occupation $\hat{n}$ of excess electrons on the metallic island. Specifically, we assume that the electron-vibron coupling does not break the underlying parity symmetry of the vibronic dynamics under $X \to -X$. This follows naturally when the coupling emerges from the electron-phonon coupling *intrinsic* to the nanobeam[20] and implies that the coupling depends only on even powers of the vibronic mode coordinate X. The dominant coupling is quadratic in X,

$$H_c = \frac{g}{2}X^2\hat{n}, \qquad (2)$$

with a coupling constant $g > 0$.[20] When there is a significant contribution to the electron-vibron coupling originating from the electrostatic dot-gate interaction, we envision a symmetric gate setup consistent with Eq. (2).

In the presence of the vibronic dynamics $X(t)$, the electronic occupation $n(X,t)$ of the island is described by the Boltzmann-Langevin equation[21]

$$\frac{dn}{dt} = \{n, H_{\text{vib}}\} + \Gamma_+(1-n) - \Gamma_- n + \delta J_+ - \delta J_-. \qquad (3)$$

This equation assumes that the bias is large compared to temperature so that tunneling is effectively unidirectional and the relevant tunneling rates $\Gamma_\pm$ for tunneling onto (+) and off (−) the island are given by $\Gamma_\pm = R^{-1}(V/2 \pm \bar{V}_g)\Theta(V/2 \pm \bar{V}_g)$. Here, R denotes the tunneling resistances ($R \gg h/e^2$) between island and leads, V is the bias voltage, $\Theta(x)$ denotes the Heaviside step function, and we set $\hbar = e = 1$. Since both gate voltage [via the capacitances C and C_g in Fig. 1(c)] and vibronic deformations couple to the excess charge $\hat{n}$ on the island, the effective gate voltage $\bar{V}_g = V_g - gX^2/2$ combines the gate potential V_g (measured from the degeneracy point between the states with zero and one excess electron) and the vibron-induced shift of the electronic energy described by H_c. The stochastic Poisson nature

of electronic tunneling is accounted for by including the Langevin sources $\delta J_\pm$ with correlators $\langle \delta J_+(t)\delta J_+(t')\rangle = \Gamma_+(1-n)\delta(t-t')$ and $\langle \delta J_-(t)\delta J_-(t')\rangle = \Gamma_- n\delta(t-t')$. The vibronic dynamics enters Eq. (3) through the Poisson bracket $\{n, H_{\text{vib}}\}$.

III. STABILITY ANALYSIS

We are now in a position to investigate the influence of the electronic dynamics on the vibronic motion. Near the instability, the vibrational dynamics becomes slow compared to the electronic tunneling dynamics. As has recently been shown,[22,23] the effect of the current on the vibrational motion can then be described within a NEBO approximation in which the vibrational motion is subject to a current-induced force $-gXn(X,t)$ originating in the electron-vibron interaction (2). This current-induced force involves both a time-averaged and conservative force as well as fluctuating and frictional forces, resulting in Langevin dynamics of the vibronic degree of freedom.

In lowest order, the Langevin dynamics only involves the conservative force which emerges from the average occupation $n_0(X)$ in the absence of fluctuations ($\delta J_\pm \simeq 0$) and vibronic dynamics ($\{n, H_{\text{vib}}\} \simeq 0$). In this limit, Eq. (3) reduces to the usual rate equation of a metallic SET so that[19]

$$n_0(x) = \begin{cases} 1, & v_g(x) > v/2, \\ \dfrac{1}{2} + \dfrac{v_g(x)}{v}, & -v/2 \leq v_g(x) \leq v/2, \\ 0, & v_g(x) < -v/2 \end{cases} \qquad (4)$$

with $v > 0$ and $v_g(x) = v_g - x^2/2$. Here and below, we employ dimensionless variables by introducing characteristic scales $E_0 = g^2/\alpha$ of energy, $l_0 = \sqrt{g/\alpha}$ of length, and $\omega_0 = \sqrt{g/m}$ of frequency (or time t) from a comparison of the quartic vibron potential in H_{vib} and the electron-vibron coupling H_c. Specifically, we introduce the reduced variables $x = X/l_0$, $p = P/m\omega_0 l_0$, $\tau = \omega_0 t$, $v = V/E_0$, $v_g = V_g/E_0$, and $r = R\omega_0/E_0$. In terms of these variables, we can also write $H_{\text{vib}} + H_c = E_0[p^2/2 + (-\epsilon + \hat{n})x^2/2 + x^4/4]$ in terms of a reduced compressional force $\epsilon = -m\omega^2/g$.

The current-induced force $-xn_0(x)$ has dramatic effects on the Euler instability, as follows from a stability analysis of the vibrational motion. The (meta)stable positions of the nanobeam are obtained by setting the effective force $f_{\text{eff}}(x) = \epsilon x - x^3 - xn_0(x)$ to zero. Our results are summarized in the stability diagrams in Fig. 2. The most striking results of this analysis are: (i) the current flow renormalizes the critical force required for buckling toward larger values. (ii) At low biases, the buckled state can appear via a discontinuous transition.

These results can be understood most directly in terms of the potential $v_{\text{eff}}(x)$ associated with $f_{\text{eff}}(x)$. Focusing on the current-carrying region (shown in gray in Fig. 2 and delineated by $\max\{0, \epsilon_-\} < x^2 < \epsilon_+$ with $\epsilon_\pm = 2v_g \pm v$), we find that

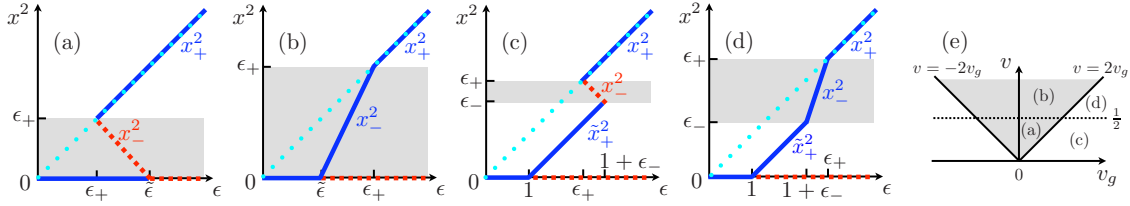FIG. 2. (Color online) (Meta)stable (solid blue lines) and unstable (dashed red lines) positions of the nanobeam vs scaled force ϵ for (a) $|v_g| < v/2$, $v < 1/2$, (b) $|v_g| < v/2$, $v > 1/2$, (c) $v_g > v/2$, $v < 1/2$ (for $\epsilon_+ > 1$; a similar plot holds for $\epsilon_+ < 1$), and (d) $v_g > v/2$, $v > 1/2$, as indicated in the v_g-v plane in (e). The dotted blue line is the result without electron-vibron coupling. Notation: $\epsilon_\pm = 2v_g \pm v$, $\tilde{\epsilon} = 1/2 + v_g/v$, $x_+^2 = \epsilon$, $\tilde{x}_+^2 = \epsilon - 1$, and $x_-^2 = (\epsilon - \tilde{\epsilon})/(1 - 1/2v)$. Grey indicates conducting regions.

$$v_{\text{eff}}(x) = \frac{1}{2}\left(-\epsilon + \frac{v + 2v_g}{2v}\right)x^2 + \frac{1}{4}\left(1 - \frac{1}{2v}\right)x^4. \quad (5)$$

The quadratic term shows that the current indeed stabilizes the unbuckled state, renormalizing the critical force to $\tilde{\epsilon} = 1/2 + v_g/v$ when $\epsilon_- < 0 < \epsilon_+$ [Figs. 2(a) and 2(b)]. Remarkably, however, the current-induced contribution to the quartic term is negative at small x^2 and thus *destabilizes* the unbuckled state. According to Eq. (5), the quartic term in the current-induced potential becomes increasingly significant as the bias voltage v decreases and we find that the overall prefactor of the quartic term becomes *negative* when $v < 1/2$.[24] It is important to note that this does not imply a globally unstable potential since the current-induced force contributes only for small x^2. A sign reversal of the quartic term is also a familiar occurrence in the Landau theory of tricritical points which connect between second- and first-order transition lines.[25] In close analogy, the sign reversal of the quartic term in the effective potential (5) signals a discontinuous Euler instability which reverts to a continuous transition at biases $v > 1/2$ where the prefactor of the quartic term remains positive.

Specifically, when $v > 1/2$ [Figs. 2(b) and 2(d)], the current-induced potential renormalizes the parameters of the vibronic Hamiltonian but leaves the quartic term positive. This modifies how the position of the minimum depends on the applied force in the conducting region $\max\{0, \epsilon_-\} < x^2 < \epsilon_+$, but the Euler instability remains continuous. When $v < 1/2$, the equilibrium position at finite x becomes unstable within the entire current-carrying region. This leads to a discontinuous Euler transition when $\epsilon_- < 0 < \epsilon_+$ [Fig. 2(a)] and to multistability in the region $\epsilon_- < x^2 < \epsilon_+$ when $\epsilon_- > 0$ [Fig. 2(c)].[26]

At the level of the stability analysis, we can also obtain the current I by evaluating the rate-equation result[19] $RI(x)/V = 1/4 - [v_g(x)/v]^2$ at the position of the most stable minimum. Corresponding results in the v_g-v plane are shown in Figs. 3(a)–3(f) for various values of the applied force ϵ. By comparison with the Coulomb diamond in the absence of the electron-vibron coupling (dotted lines in Fig. 3), we see that the Euler instability leads to a current blockade over a significant parameter range. For $v > 1/2$, the blockade is a manifestation of the Franck-Condon blockade,[15,17] caused by the induced linear electron-vibron coupling when expanding Eq. (2) about the buckled state.

In contrast, for $v < 1/2$, the current blockade is a direct consequence of the discontinuous Euler instability. We have

seen above that in this regime, the buckled state becomes unstable throughout the entire current-carrying region. As a result, the current-induced force will always drive the system out of the current-carrying region, explaining the current blockade. An intriguing feature of this novel tricritical current blockade is the curved boundary of the apparent Coulomb-blockade diamond (Fig. 3), a behavior which is actually observed in nanoelectromechanical systems.

IV. LANGEVIN DYNAMICS

To investigate the robustness of the stability analysis against fluctuations, we turn to the complete vibronic Langevin dynamics $\ddot{x} + \gamma(x)\dot{x} = f_{\text{eff}}(x) + \xi(\tau)$. The fluctuating force $\xi(\tau)$ is generated by fluctuations of the electronic occupation and the frictional force $-\gamma(x)\dot{x}$ by the delayed response of the electrons to the vibronic dynamics. To compute $\gamma(x)$ and $\xi(\tau)$, we solve Eq. (3) including the vibronic dynamics and the Langevin sources. Writing separate equations for average and fluctuations of the occupation by setting $n = \bar{n} + \delta n$, we
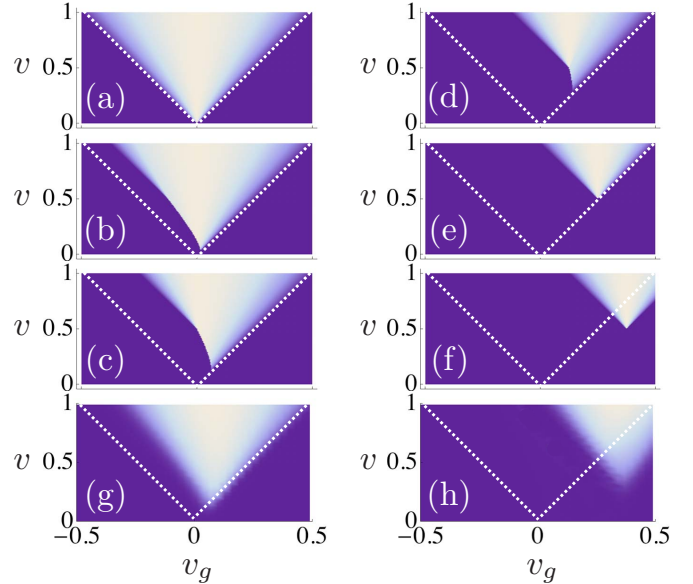

FIG. 3. (Color online) Conductance $G = RI/V$ in the v_g-v plane for applied force (a) $\epsilon \leq 0$, (b) $\epsilon = 0.25$, (c) and (g) $\epsilon = 0.5$, (d) $\epsilon = 0.75$, (e) $\epsilon = 1$, and (f) and (h) $\epsilon = 1.25$, within (a)–(f) stability analysis and (g) and (h) full Langevin dynamics ($r = \gamma_e = T = 0.01$). Color scale: $G = 0 \rightarrow 1/4$ from dark blue to white. Dotted lines delineate the Coulomb diamond for $g = 0$.

see that the leading correction to $\bar{n}$ arises from the Poisson bracket, yielding $\bar{n}=n_0-\frac{1}{\Gamma_++\Gamma_-}\dot{X}\partial_X n_0$. At the same time, the fluctuations δn obey the correlator $\langle\delta n(t)\delta n(t')\rangle=\frac{2}{\Gamma_++\Gamma_-}n_0(1-n_0)\delta(t-t')$. Inserting these results into the expression for the current-induced force $-gXn$ and employing reduced units, we find $\langle\xi(\tau)\xi(\tau')\rangle=D(x)\delta(\tau-\tau')$ with diffusion and damping coefficients $D(x)=2rx^2n_0(1-n_0)/v$ and $\gamma(x)=-rx\partial_x n_0/v$, respectively. Finally, we can pass from the Langevin to the equivalent Fokker-Planck equation[22,23] for the probability $\mathcal{P}(x,p,\tau)$ that the nanobeam is at position x and momentum p at time τ,

$$\partial_\tau\mathcal{P}=-p\partial_x\mathcal{P}-f_{\mathrm{eff}}\partial_p\mathcal{P}+\gamma\partial_p(p\mathcal{P})+\frac{D}{2}\partial_p^2\mathcal{P}. \quad (6)$$

Note that the diffusion and damping coefficients are nonvanishing only in the conducting region.[27]

The current $I=\int dxdp\mathcal{P}_{\mathrm{st}}(x,p)I(x)$ is now obtained from the stationary solution $\partial_\tau\mathcal{P}_{\mathrm{st}}=0$ of the Fokker-Planck Eq. (6). Numerical results for the scaled linear conductance $G=RI/V$ are shown in Figs. 3(g) and 3(h), using the same parameters as in Figs. 3(c) and 3(f). We observe that the fluctuations reduce the size of the blockaded region and blur the edges of the conducting regions as the system can explore more conducting states in phase space. Nevertheless, the conclusions of the stability analysis clearly remain valid qualitatively.

V. CONCLUSION

We have presented a general approach to the interplay between continuous mechanical instabilities and current flow in nanoelectromechanical systems, and have applied our general framework to the Euler buckling instability. The current flow modifies the nature of the buckling instability from a continuous to a tricritical transition. Likewise, the instability induces a novel tricritical current blockade at low bias. Our nonequilibrium Born-Oppenheimer approach generalizes not only to other continuous mechanical instabilities but also to other systems such as semiconductor quantum dots or single-molecule junctions with a discrete electronic spectrum, to other types of electron-vibron coupling[28] and to further transport characteristics (e.g., current noise).

Our setup can be realized experimentally by clamping, e.g., a suspended carbon nanotube and applying a force to atomic precision either using a break junction or an atomic force microscope. Indeed, several recent experiments show that the electron-vibron coupling is surprisingly strong in suspended carbon nanotube quantum dots.[4,5,16]

[1] L. D. Landau and E. M. Lifshitz, *Theory of Elasticity* (Pergamon Press, Oxford, 1970).

[2] L. Euler, in *Leonhard Euler's Elastic Curves*, edited by W. A. Oldfather, C. A. Ellis, and D. M. Brown, ISIS No. 58 XX(1) (Saint Catherine Press, Bruges, 1744).

[3] P. Poncharal *et al.*, Science **283**, 1513 (1999).

[4] G. A. Steele *et al.*, Science **325**, 1103 (2009).

[5] B. Lassagne *et al.*, Science **325**, 1107 (2009).

[6] M. R. Falvo *et al.*, Nature (London) **389**, 582 (1997).

[7] S. M. Carr and M. N. Wybourne, Appl. Phys. Lett. **82**, 709 (2003).

[8] W. Bao *et al.*, Nat. Nanotechnol. **4**, 562 (2009).

[9] J. C. Meyer *et al.*, Nature (London) **446**, 60 (2007).

[10] S. M. Carr, W. E. Lawrence, and M. N. Wybourne, Phys. Rev. B **64**, 220101(R) (2001).

[11] P. Werner and W. Zwerger, Europhys. Lett. **65**, 158 (2004).

[12] V. Peano and M. Thorwart, New J. Phys. **8**, 21 (2006).

[13] S. Savel'ev, X. Hu, and F. Nori, New J. Phys. **8**, 105 (2006).

[14] H. G. Craighead, Science **290**, 1532 (2000); M. L. Roukes, Phys. World **14**, 25 (2001).

[15] J. Koch and F. von Oppen, Phys. Rev. Lett. **94**, 206804 (2005).

[16] R. Leturcq *et al.*, Nat. Phys. **5**, 327 (2009).

[17] F. Pistolesi and S. Labarthe, Phys. Rev. B **76**, 165317 (2007).

[18] The rotation of the plane of the buckled nanobeam is assumed massive due to clamped boundary conditions.

[19] See, e.g., T. Dittrich *et al.*, *Quantum Transport and Dissipation* (Wiley-VCH, Weinheim, 1998), Chap. 3.

[20] E. Mariani and F. von Oppen, Phys. Rev. B **80**, 155411 (2009).

[21] See Ya. M. Blanter and M. Buttiker, Phys. Rep. **336**, 1 (2000), for a review of the Boltzmann-Langevin method.

[22] Ya. M. Blanter, O. Usmani, and Yu. V. Nazarov, Phys. Rev. Lett. **93**, 136802 (2004); **94**, 049904(E) (2005).

[23] D. Mozyrsky, M. B. Hastings, and I. Martin, Phys. Rev. B **73**, 035104 (2006).

[24] We note that the singularity at small v is cutoff for bias voltages of the order of temperature or level broadening.

[25] See, e.g., P. M. Chaikin and T. C. Lubensky, *Principles of Condensed Matter Physics* (Cambridge University Press, Cambridge, 1995).

[26] In a quite different context, a discontinuous Euler instability has also been predicted in S. Savel'ev and F. Nori, Phys. Rev. B **70**, 214415 (2004).

[27] In some cases, a stable numerical solution of Eq. (6) requires a small extrinsic damping γ_e and temperature T.

[28] E.g., a small symmetry-breaking coupling linear in X leads to a tricritical point in an external field, a purely linear coupling to a second-order transition in a field, G. Weick *et al.* (unpublished).